Einstein on the beach
fluid flow on a curved space

Jean-Luc Thiffeault

Department of Mathematics
University of Wisconsin – Madison

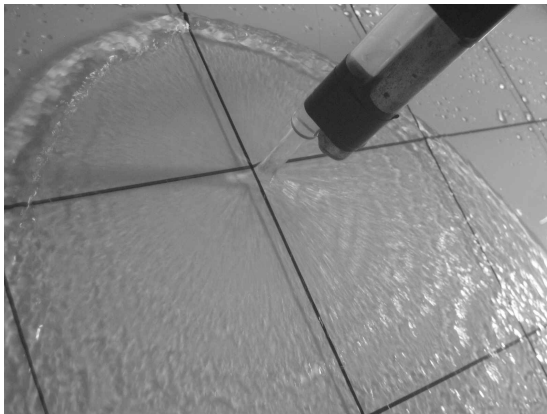with Andrew Belmonte (Penn State), Khalid Kamhawi, and Jay Johnson (UW)

Sydney Dynamics Group Seminar
University of Sydney, 29 August 2014

WISCONSIN
UNIVERSITY OF WISCONSIN–MADISON

Plane inclined at 45°. The flow rate is $Q \simeq 120 \, \mathrm{cm^3 \, s^{-1}}$.

[with Andrew Belmonte in Claudia Cenedese and Karl Helfrich's lab at Woods Hole, GFD 2008]

Try steady potential flow: $\mathbf{u} = \nabla\varphi$, with

$$\nabla^2\varphi = 0, \qquad \text{mass conservation;}$$
$$\tfrac{1}{2}\left|\nabla\varphi\right|^2 + \frac{p}{\rho} - \mathbf{g}\cdot\mathbf{r} = H, \qquad \text{Bernoulli's law;}$$

Boundary conditions:

$$\partial_z\varphi = 0 \qquad \text{at } z = 0, \qquad \text{no-throughflow at substrate;}$$
$$\nabla\varphi\cdot\nabla h = \partial_z\varphi \quad \text{at } z = h, \qquad \text{kinematic condition at free surface;}$$
$$p = 0 \qquad \text{at } z = h, \qquad \text{constant pressure at free surface.}$$

Here z is normal to the substrate, x_1 and x_2 are parallel to it.

Small-parameter expansion

Expand Bernoulli's law in the small fluid depth ε:

$$\sum_{j=1}^{2} (\partial_j \varphi)^2 + \varepsilon^{-2}(\partial_z \varphi)^2 + \frac{2p}{\rho} - 2\mathbf{g} \cdot (\mathbf{X} + \varepsilon\, z\, \hat{\mathbf{e}}_3) = 2H,$$

where $\mathbf{X} = x_1 \hat{\mathbf{e}}_1 + x_2 \hat{\mathbf{e}}_2$. Also expand φ:

$$\varphi(x_1, x_2, z) = \varphi_{(0)} + \varepsilon\, \varphi_{(1)} + \varepsilon^2\, \varphi_{(2)} + \ldots,$$

to obtain at leading order $\partial_z \varphi_{(0)} = 0$, so that

$$\varphi_{(0)} = \Phi(x_1, x_2).$$

At next order:

$$\sum_{j=1}^{2}(\partial_j\Phi)^2 + (\partial_z\varphi_{(1)})^2 + \frac{2p}{\rho} - 2\mathbf{g}\cdot\mathbf{X} = 2H,$$

Evaluate at $z = h$ and use the boundary conditions:

$$\sum_{j=1}^{2}(\partial_j\Phi)^2 - 2\mathbf{g}\cdot\mathbf{X} = 2H,$$

Solution in terms of characteristics

Differentiate to get rid of constant:

$$\sum_{j=1}^{2} \partial_j \Phi \, \partial_{ij} \Phi = \mathbf{g} \cdot \partial_i \mathbf{X}, \qquad i = 1, 2.$$

Introduce the characteristics $x_1(\tau)$, $x_2(\tau)$:

$$\dot{x}_1 = \partial_1 \Phi(\mathbf{x}), \qquad \dot{x}_2 = \partial_2 \Phi(\mathbf{x}),$$

We have $\partial_{ij} \Phi = \partial_i \dot{x}_j$ and $\ddot{x}_i = (\partial_j \dot{x}_i) \dot{x}_j = \partial_j \Phi \, \partial_{ij} \Phi$, so that
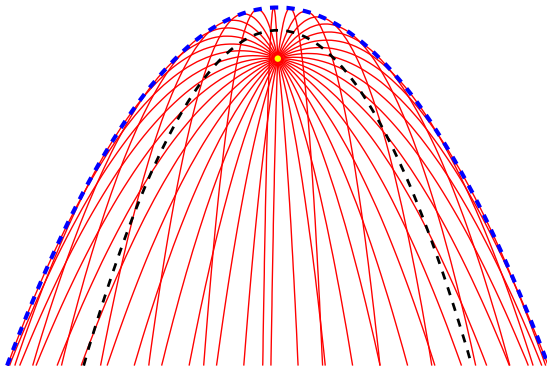
$$\ddot{x}_i = \mathbf{g} \cdot \hat{\mathbf{e}}_i, \qquad i = 1, 2.$$

[Rienstra (1996)]

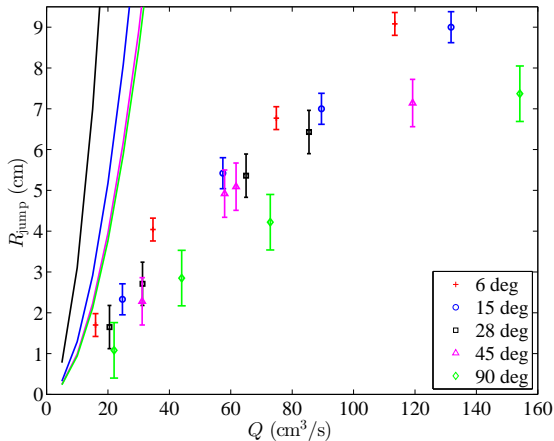The characteristics have a parabolic envelope (blue dashed):

Edwards *et al.* (2008) used the 'delta-shock' framework to account for characteristics crossing: this lowers the rise distance by 5/9, and the profile remains essentially parabolic (black dashes).

Compare ballistic rise distance $U^2/2g\sin\theta$ to experiments:
[Thiffeault & Belmonte (2010)]

Not so good... even if we lower the curves by 5/9 following Edwards *et al.* (2008).

- Watson (1964): inviscid and viscid, but assumes position of jump.
- Many subsequent refinements: Bohr *et al.* (1993); Godwin (1993); Bohr *et al.* (1997); Brechet & Néda (1999); Chang *et al.* (2001); Bush & Aristoff (2003)....
- Jet striking a horizontal plate at an oblique angle: Sparrow & Lovell (1980); Rubel (1981); Kate *et al.* (2007).
- Jet striking a moving plate: Gradeck *et al.* (2006); Kate *et al.* (2009).
- Microdecorated surface: Dressaire *et al.* (2009).
- Here we'll adapt the model of Bohr *et al.* (1993) to an inclined plane. Our main assumption is that, as far as the rise distance is concerned, the jet is 'locally' circular.

A simple model with viscosity

Let's cheat and assume that the jet is hitting an inverted cone, so that the system is axially-symmetric.

Following Bohr *et al.* (1993), start with boundary layer equations:

$$u\frac{\partial u}{\partial r} + w\frac{\partial u}{\partial z} = -g\cos\theta\frac{dh}{dr} - g\sin\theta + \nu\frac{\partial^2 u}{\partial z^2}$$

$$\frac{\partial u}{\partial r} + \frac{u}{r} + \frac{\partial w}{\partial z} = 0$$

where $u(r, z)$ and $w(r, z)$ are respectively the velocity components tangent and perpendicular to the solid surface.

r is tangent to the solid surface, and z is perpendicular to it.

A simple model with viscosity II

The boundary conditions at the bottom and top of the fluid are

$$u = 0, \quad w = 0, \qquad \text{at } z = 0;$$

$$\frac{\partial u}{\partial z} = 0, \quad w = u\,\frac{dh}{dr}, \qquad \text{at } z = h(r).$$

Integrating gives the mass conservation equation

$$r \int_0^h u(r, z)dz = q$$

where $q = Q/2\pi$, with Q the flow rate of the jet.

In addition, we must specify the velocity $u(r_0, z) = u_0(z)$ and height $h(r_0) = h_0$ at a radius r_0 larger than the jet radius, since the boundary layer equations are not valid directly under the jet.

We use the standard hydraulic jump scalings to define dimensionless 'tilde' variables:

$$
\begin{aligned}
u &= \alpha \tilde{u}, & \alpha &= (c_1^{-1/2} c_2^{1/8})\, q^{1/8} \nu^{1/8} (g \cos\theta)^{3/8}, \\
w &= \beta \tilde{w}, & \beta &= \phantom{(c_1^{1/2} c_2^{-3/8})}\, q^{-1/4} \nu^{3/4} (g \cos\theta)^{1/4}, \\
r &= \Gamma \tilde{r}, & \Gamma &= (c_1^{1/2} c_2^{-3/8})\, q^{5/8} \nu^{-3/8} (g \cos\theta)^{-1/8}, \\
z &= \delta \tilde{z}, & \delta &= (c_2^{1/4})\, \phantom{c_1^{1/2}}\, q^{1/4} \nu^{1/4} (g \cos\theta)^{-1/4},
\end{aligned}
$$

except that we included the $\cos\theta$ dependence in the scalings.

We immediately drop the tildes.

(We will discuss the dimensionless constants c_1 and c_2 below.)

Upon averaging in the z direction, the boundary-layer equation becomes after integration by parts

$$2u\overline{\frac{\partial u}{\partial r}} + \frac{1}{r}\overline{u^2} + \frac{h'}{h}\left.u^2\right|_{z=h} = -c_1\left(G + \frac{dh}{dr}\right) - \frac{c_1}{c_2}\frac{1}{h}\left.\frac{\partial u}{\partial z}\right|_{z=0}$$

where the z-average of a function $F(r,z)$ is

$$\overline{F}(r) = (1/h)\int_0^h F(r,z)dz$$

and we defined

$$G = (c_1^{1/2}c_2^{-5/8})\,q^{3/8}\nu^{-5/8}(g\cos\theta)^{1/8}\tan\theta\,.$$

We now assume the separable form

$$u(r, z) = v(r)f'(z/h(r)),$$

where $v = \overline{u}$ is the averaged profile, f is a given function that describes the vertical structure of the thin layer, with $f(0) = f'(0) = f''(1) = 0$, $f(1) = 1$.

Mass conservation integral becomes simply $vhr = 1$, which gives a relationship between v and h. This allows us to derive the two relations

$$2\overline{u\frac{\partial u}{\partial r}} + \frac{1}{r}\,\overline{u^2} + \frac{h'}{h}\,u^2\big|_{z=h} = c_1\,v\frac{\partial v}{\partial r}, \qquad \frac{\partial u}{\partial z}\bigg|_{z=0} = c_2\,\frac{v}{h},$$

with

$$c_1 = \int_0^1 f'^2(\eta)d\eta \qquad \text{and} \qquad c_2 = f''(0).$$

The two relations can be used in the earlier averaged equations to obtain

$$vv' + h' = -\frac{v}{h^2} - G, \qquad vhr = 1.$$

For $G = 0$ these reduce to the equations of Bohr *et al.* (1993), which are essentially as derived by Kurihara (1946) and Tani (1949).

Combine into one ODE for $v(r)$:

$$r(1 - rv^3)v' = -(1 - Gr^2v - r^4v^4)v,$$

which must be solved together with the flux boundary condition $v(r_0) = v_0$ at the jet radius r_0.

$$r(1 - rv^3)v' = -(1 - Gr^2v - r^4v^4)v$$

Singularity at $rv^3 = 1$ will determine the location of the hydraulic jump ($v' \to -\infty$), which we will associate here with the rise distance.

Since $G = G(Q, \theta)$, this ODE will have to be solved at each inclination angle and flow rate.

When doing numerical calculations, use the parabolic profile

$$f(\eta) = \tfrac{3}{2}\eta^2 - \eta^3,$$

from which $c_1 = 6/5$, $c_2 = 3$. A more general approach, using a variable cubic profile as in Bohr *et al.* (1997), doesn't much change the scaling.

Numerical solution

For $Q \simeq 119 \text{ cm}^3 \text{ s}^{-1}$ and $\theta = 45°$:
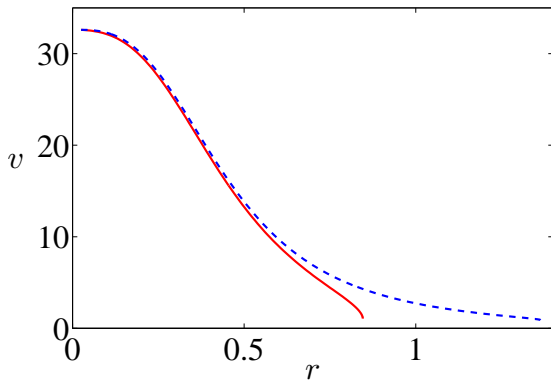
Solid red: $G = 67$; blue dashed: $G = 0$.

(Fairly insensitive to jet radius r_0.)

This overestimates the rise height, unsurprisingly:
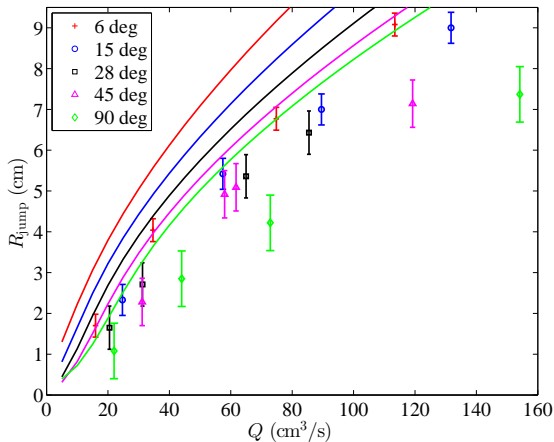
But the scaling looks pretty good...

Corrected model

Let's cheat and multiply by fitted parameter 0.76, to adjust for the singularity position occuring beyond the actual jump:
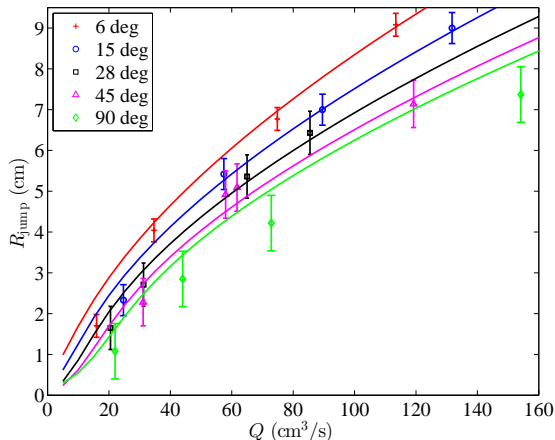
Not so bad..., except at 90° (vertical wall). [Thiffeault & Belmonte (2010)]

Rienstra (1996) also applied his inviscid model to curved surfaces (spheres, cylinders). Here's my attempt at an experiment [Thiffeault & Kamhawi (2008)]:

Compare to characteristics on a cylinder:

General curved substrates

Rienstra (1996) treated surfaces with global orthogonal coordinates (plane, cylinder, sphere).

What about more general surfaces?

Write x^1, x^2 for general 2D coordinates that locate a point on the substrate. A small-thickness expansion similar to Rienstra's yields for the characteristics [Thiffeault & Kamhawi (2008)]:

$$\ddot{x}^\sigma + \Gamma^\sigma_{\alpha\beta}\,\dot{x}^\alpha\dot{x}^\beta = \mathbf{g} \cdot \mathbf{e}^\sigma$$

where $\Gamma^\sigma_{\alpha\beta}$ are the Christoffel symbols for the shape of the substrate.

This is the geodesic equation with a gravitational forcing. The fluid particles (characteristics) are trying to follow straight lines, but their trajectories are bent by the substrate curvature and gravity.

The geodesic equations are actually a fourth-order autonomous system.

Hence, chaos is a possibility, as long as the substrate does not possess a continuous symmetry! (Ruled out for plane, cylinder, sphere.)

Consider a simple substrate shape parametrized by:
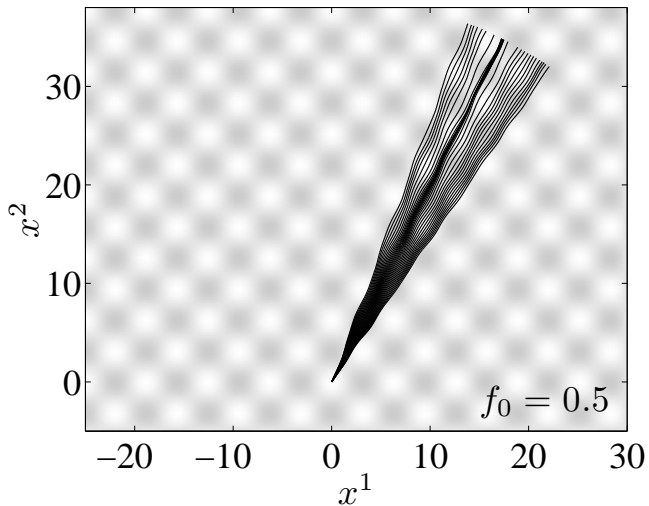
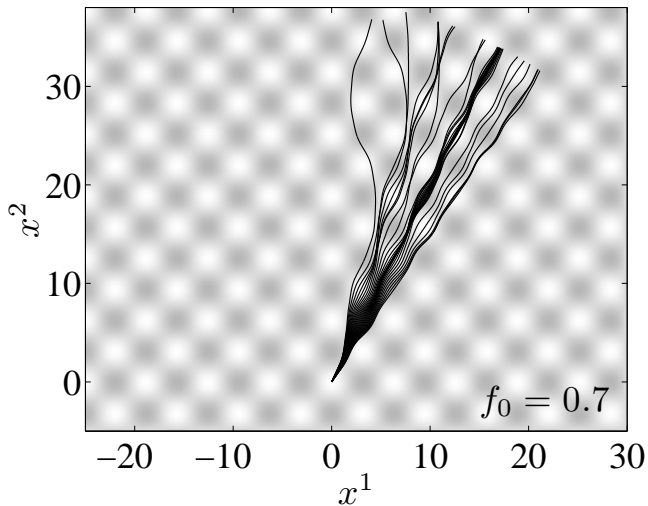$$f(x^1, x^2) = f_0 \cos x^1 \cos x^2$$
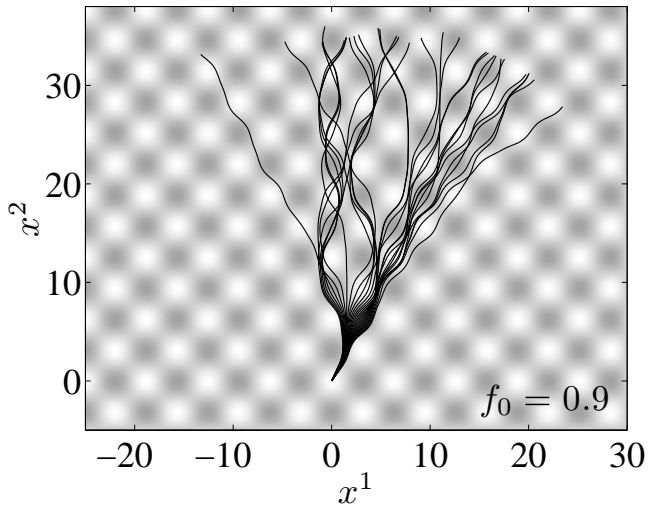
First take $g = 0$ and keep the surface horizontal.
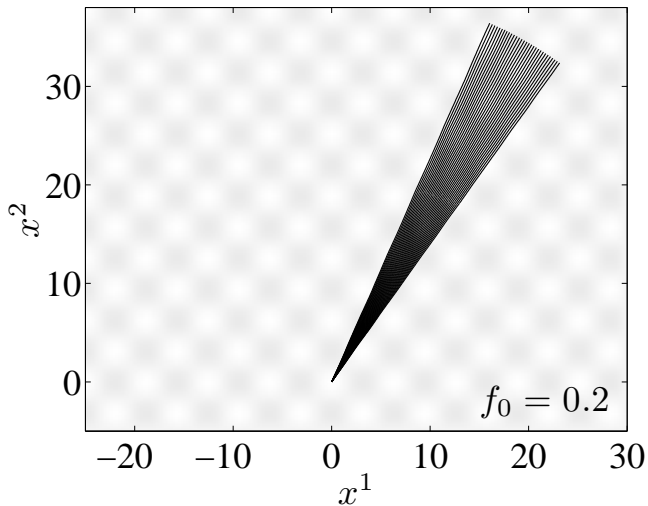
$f_0 = 0.7$

$f_0 = 0.9$

$f_0 = 1.0$
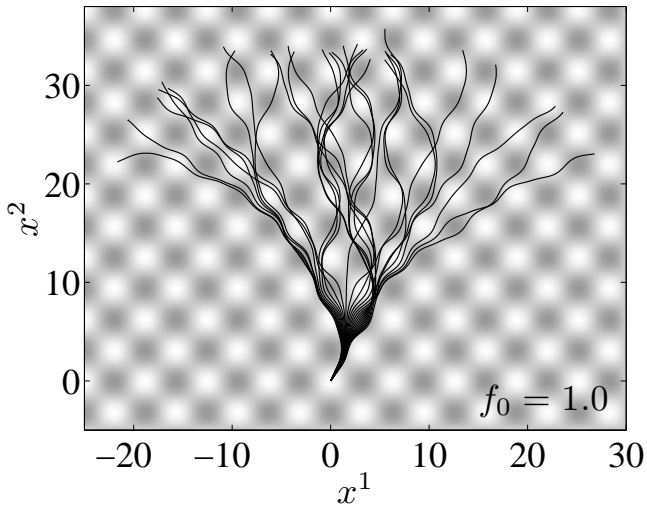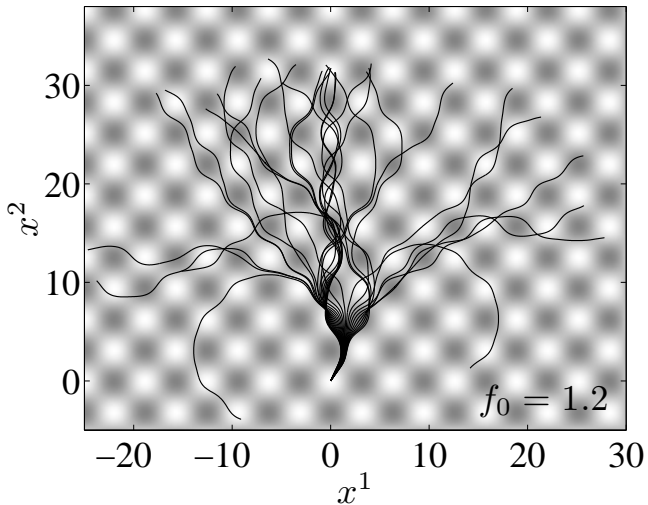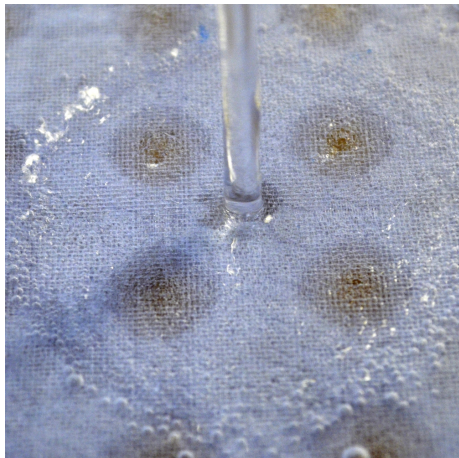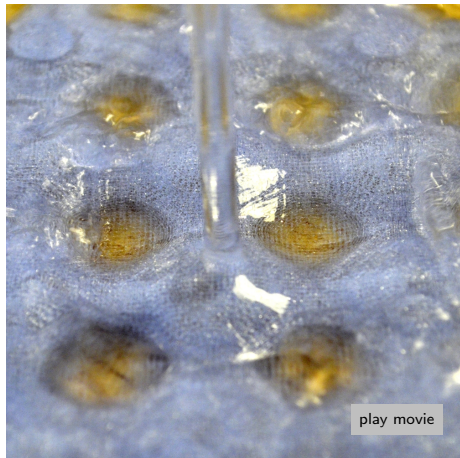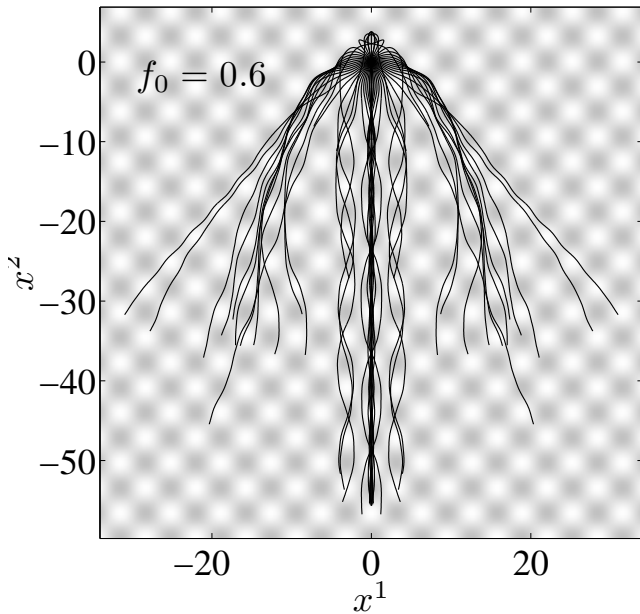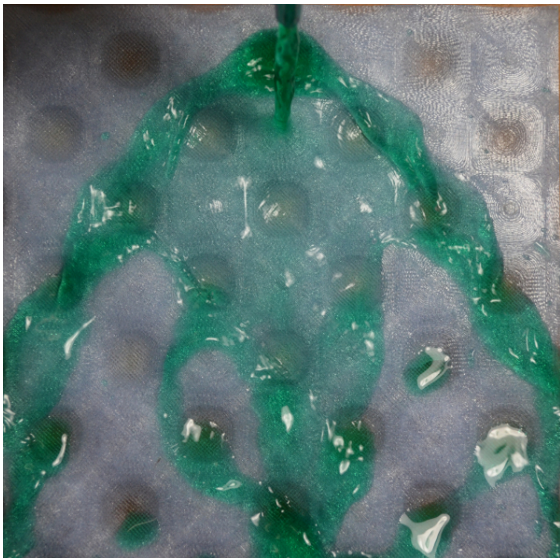
Flat substrate

Patterned substrate

Jump is about 50% larger for a flat substrate. [Experiments with Jay Johnson.]

The simple model correctly predicts the multiple 'paths'.

Thank you!

References I

Bohr, T., Dimon, P., & Putkaradze, V. (1993). *J. Fluid Mech.* **254**, 635–648.

Bohr, T., Putkaradze, V., & Watanabe, S. (1997). *Phys. Rev. Lett.* **79** (6), 1038–1041.

Brechet, Y. & Néda, Z. (1999). *Am. J. Phys.* **67** (8), 723–731.

Bush, J. W. M. & Aristoff, J. M. (2003). *J. Fluid Mech.* **489**, 229–238.

Chang, H.-C., Demekhin, E. A., & Takhistov, P. V. (2001). *Journal of Colloid and Interface Science,* **233**, 329–338.

Dressaire, E., Courbin, L., Crest, J., & Stone, H. A. (2009). *Phys. Rev. Lett.* **102** (19), 194503.

Edwards, C. M., Howison, S. D., Ockendon, H., & Ockendon, J. R. (2008). *IMA J. Appl. Math.* **73** (1), 137–157.

Godwin, R. P. (1993). *Am. J. Phys.* **61** (8), 829–832.

Gradeck, M., Kouachi, A., Dani, A., Amoult, D., & Boréan, J. L. (2006). *Exp. Therm. Fluid Sci.* **30**, 193–201.

Kate, R. P., Das, P. K., & Chakraborty, S. (2007). *J. Fluid Mech.* **573**, 247–263.

Kate, R. P., Das, P. K., & Chakraborty, S. (2009). *J. Fluids Eng.* **131** (3), 034502.

Kurihara, M. (1946). *Rep. Research Institute for Fluid Engineering (Kyusyu Imperial University, "Ryutai Kougaku Kenkyusho Kiyou"),* **3**, 11–33. in Japanese.

Rienstra, S. W. (1996). *Z. Angew. Math. Mech.* **76** (S5), 423–424.

Rubel, A. (1981). *AIAA J.* **19**, 863–871.

Sparrow, E. M. & Lovell, B. J. (1980). *ASME, Ser. C: J. Heat Transfer,* **102**, 202–209.

Tani, I. (1949). *J. Phys. Soc. Japan,* **4**, 212–215.

Thiffeault, J.-L. & Belmonte, A. (2010). arXiv:1009.0083.

Thiffeault, J.-L. & Kamhawi, K. (2008). In: *Chaos, Complexity, and Transport: Theory and Applications*, (Chandre, C., Leoncini, X., & Zaslavsky, G., eds) pp. 40–54, Singapore: World Scientific.

Watson, E. J. (1964). *J. Fluid Mech.* **20** (3), 481–499.